JOURNAL OF CATALYSIS 101, 484–495 (1986)

Texture and Surface Chemistry of Aluminum Phosphates

J. M. CAMPELO,* J. M. MARINAS,* S. MENDIOROZ,† AND J. A. PAJARES†

*Departamento de Química Orgánica, Universidad de Córdoba, and †Instituto de Catálisis y Petroleoquímica, CSIC, Serrano, 119, 28006 Madrid

Received June 3, 1985; revised May 29, 1986

Chemical composition, texture, and surface reactivity of three samples of aluminum phosphate prepared by aging of aluminum chloride and orthophosphoric acid in different media (aqueous ammonia, ethylene, and propylene oxide) have been studied. The final pH value, 6.1, was the same in the three procedures. The Al/P molar ratio was near stoichiometry (0.86–1.22). Although the samples were heated to temperatures as high as 1000°C, X-ray diffractograms gave lines corresponding only to $AlPO_4$. Significant differences in texture and mainly in concentration of surface acidic, basic, and redox centers, were found, showing that the nature of the precipitating agent also plays an important role in determining the final properties of the high area, near stoichiometric aluminum phosphate obtained.

INTRODUCTION

In this paper extended data on texture characterization and surface chemical reactivity of three different preparations of near stoichiometric $AlPO_4$ are given. Aluminum phosphate has been reported to be active both in liquid phase hydrogenation (*1*) and acid-base catalysis (*2–6*).

The texture and surface chemistry of $AlPO_4$ has been treated among others, in the excellent review by Moffat (*2*) and in a more recent paper by Haber and Szybalska (*4*). $AlPO_4$ belongs to a family of compounds whose network, due to the covalent character of phosphorus, ranges from more or less irregular open cylindrical pores, as in silica, to classic lamellar structures (*2*). Indeed, the chemical formula of the new AlPO family of zeolites (*7, 8*) falls within the range of aluminum phosphate preparations.

The methods of preparation of high surface area $AlPO_4$ usually follow a variant of the procedure first described by Kearby (*9*), i.e., gelification of a mixture of an aluminum salt (chloride, nitrate) with orthophosphoric acid (or NaH_2PO_4 (*4*)) in the presence of a base (ethylene oxide (*9, 10*), propylene oxide (*10*), ammonia (*1, 3, 5, 6*)). By changing the relative proportions of the reactants a series of preparations can be obtained, whose Al/P ratio can vary from near zero to 20 (*2, 4, 1*).

Recently, some controversy has arisen in this journal (*11, 12, 6*) starting with the statement of Vogel and Marcelin (*11*) that near stoichiometric Al/P preparations carried out at pH > 4 are not aluminum phosphate but rather an alumina–aluminum phosphate (AAP) mixture. We hope that results of this work help to clarify this issue.

EXPERIMENTAL

Materials

Three different aluminum orthophosphates were prepared by mixing aqueous solutions of $AlCl_3 \cdot 6H_2O$ and H_3PO_4 (85% wt) in stoichiometric amounts in the presence of ethylene oxide (sample B), propylene oxide (PC), and aqueous ammonia (F) as neutralizing agents. The neutralizer was added slowly dropwise with vigorous stirring in order to get a homogeneous pH through the whole solution until precipitation took place. The pH value at the precipitation end point was 6.1 in all cases.

0021-9517/86 $3.00

The precipitation was always carried out at 273 K. After allowing the obtained gel to settle, it was filtered, washed with isopropyl alcohol, and dried at 393 K for 24 h. The resulting powders were screened at 200–250 mesh and then calcined at 920 K for 3 h and stored in a desiccator. More details about the methods of preparation can be obtained from Ref. (*13*).

Apparatus and Methodology

Chemical analyses were effected with a 3030 Perkin–Elmer AA spectrometer, using conventional methods: 309.3-nm wavelength, 0.7-nm slit for Al, and 213.6-nm wavelength, 0.2-nm slit for P. In both cases a nitrous oxide–acetylene flame and a Hollow Cathode Lamp (HCL) as excitation source were used. Sensitivity was 1.1 ppm for Al and 290 ppm for P (data on P content may be affected by this poor sensitivity). X-Ray diffraction powder analyses were performed with Fe-filtered Co$K\alpha$ radiation (λ = 1.79026 Å) in a Philips X-ray diffractometer. The instrument was operated with a scanning speed of 2°/min, and data were recorded for 2θ between 10 and 80°. Eventually a speed of 1°/min was used in order to get a higher resolution of the more important peaks. TGA's were carried out in a Perkin–Elmer TGS2 thermobalance which was commanded through a Thermal Analysis Controller System 7/4. Data were collected as percentage weight loss in a Data Station 3600, which is also used as a processing system. Sensitivity of the equipment was 0.2 μg.

Conventional methods were used for textural characterization. SEM micrographs were taken with an ISI-130 microscope. Particle size distributions were determined using a Coulter counter ZM system. Nitrogen isotherms at 77 K were obtained with a Micromeritics Digisorb 2500 plus a PDP-8 microcomputer. Mercury intrusion porosimetry to 206.7 MPa (30.000 psi) was effected using a Micromeritics 9300 Pore Size Analyzer (30 Å minimum pore radius attained).

TABLE 1

Chemical Analysis and Al/P Ratios

Sample	Al%	P%	Al/P, molar ratio
B	19.64	18.55	1.22
F	19.54	23.72	0.94
PC	20.79	27.84	0.86

Various methods were used to determine surface reactivity. The presence of surface hydroxyls was studied by combined TG-IR experiments. IR spectra at room temperature were run in a PE 682 spectrometer on 2% $AlPO_4$ in KBr pressed disks (~200 mg weight, ~13 cm^2/g exposed geometrical area). Materials previously ground to 0.1 mm size, were pressed at 2, 5 and 8 $\times$ 10^3 $kg \cdot cm^{-2}$ and maintained in a desiccator until spectra were run.

Acid centers were determined by titration with cyclohexylamine (CY, pK_a = 10.6), pyridine (PY, pK_a = 5.3), and 2,6-di-t-butyl-4-methylpyridine (DTBMPY, pK_a = 7.5), and basic centers were titrated with acrylic acid (AA, pK_a = 4.25), phenol (PH, pK_a = 9.9), and 2,6-di-t-butyl-4-methylphenol (DTBMPH, pK_a = 11.1). Oxidoreducing sites were determined on the basis of adsorption on the solid surface of phenothiazine (PNTZ, ionization energy, IE = 7.13 eV) or 1,3-dinitrobenzene (DNB, electron affinity, EA = 2.21 eV). Adsorption was carried out from cyclohexane solutions (spectroscopic grade, Merck) at 298 K using a spectrophotometric method described elsewhere (*14, 15*).

RESULTS AND DISCUSSION

Chemical Identification and Structure

Chemical analysis of the solids after drying at 378 K for 16 h gave the results collected in Table 1. The chemical formulae are not far from the stoichiometric composition, showing an excess of phosphorus in samples F (5.56%) and PC (16.43%) and a deficiency (17.85%) in sample B, as compared with $AlPO_4$.

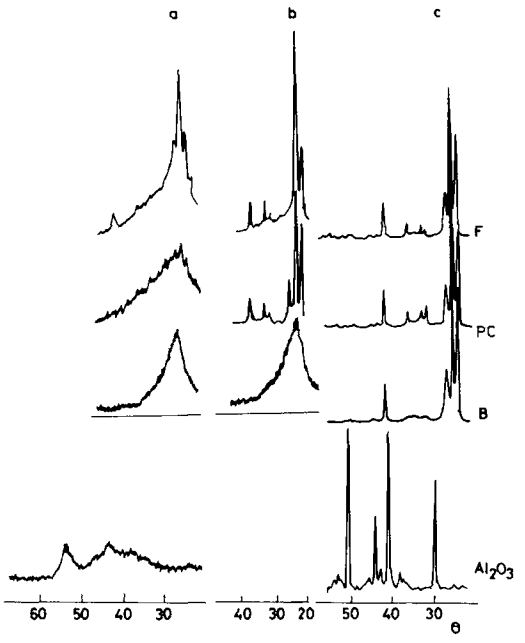

FIG. 1. X-Ray diffractograms. (a) Untreated samples, B, F, PC, Al_2O_3 (NO_3Al, NH_4OH) after 3 h, 650°C treatment. (b) After 800°C, 3 h. (c) After 1000°C, 3 h.

X-Ray diffraction patterns of the three phosphate samples, both before and after sintering in air at temperatures to 1000°C, are given in Fig. 1. From this, it is apparent that crystallinity grows with treatment temperature, but, whereas the $AlPO_4$ spectrum is fully developed at 800°C in samples PC and F, sample B needs a 4-h treatment at 1000°C for all the peaks corresponding to $AlPO_4$ to appear. Crystallinity in sample F, is fairly well developed at 650°C, growing to completion at 800°C. No signal denoting Al_2O_3 is seen. In order to compare spectra, an X-ray diffractogram for Al_2O_3 (ex $Al(NO_3)_3/NH_4OH$) previously heated at 1000°C for 3 h is also shown. After the 1000°C treatment all samples show spectra which correspond fairly well to that of ASTM synthetic $AlPO_4$, formed from $AlCl_3 \cdot 6H_2O + (NH_4)H_2PO_4$ and water heated at 950°C for 20 days, although the relative peak intensities differ slightly from those reported. The structure of samples F and PC correspond to the pseudohexagonal one of tridymite rather than to the cubic one of α-crystobalite reported by Haber and Szybalska (*4*), which is more apparent in sample B.

An aluminum phosphate prepared similarly to sample F by Itoh *et al.* (*3*) gave an amorphous X-ray pattern when heated at 750°C. Our spectra are not substantially different from those given by Vogel and Marcelin (*11*), but our interpretation differs: while they assign the crystalline material to $AlPO_4$ and the amorphous spectra to alumina–aluminum phosphate (AAP), we envisage a more simple situation, viz. a transition from an amorphous to a crystalline $AlPO_4$. Although the existence of AAP was reported by Moffat (*2*) and diffraction effects corresponding to boehmite were found by Haber and Szybalska (*4*) for preparations with $Al/P > 1.4$, the X-ray spectra obtained in this work do not show any effects different from those corresponding to $AlPO_4$ even though the treatment temperatures were high enough to produce alumina segregation. Deviations from stoichiometry fall within the range (0.8–1.2) in which the aforementioned authors (*4*) did not find either Al_2O_3 or P_2O_5 as independent components. Besides, additional experiments with $Al_2O_3 + AlPO_4$ under the same conditions (aqueous ammonia medium, pH 6.1) showed a lack of crystallinity at temperatures up to 1000°C in the Al_2O_3 and phosphate detected. The behavior was as if crystallization of these two species were mutually inhibited (Fig. 2). There is no doubt that Marcelin and Vogel's (*11*) statement, that preparation of $AlPO_4$ at pH above 4 gives AAP, cannot be generalized.

TG and DTG curves between room temperature and 1000°C for sample B as an example are given in Fig. 3. The DTG curves in static air atmosphere show a single peak at temperatures below 290°C; its size is apparently unrelated to the surface area of the samples. Above 290°C, the three samples exhibited a similar, uniform weight loss probably due to the removal of composition water, indicating similar surface states.

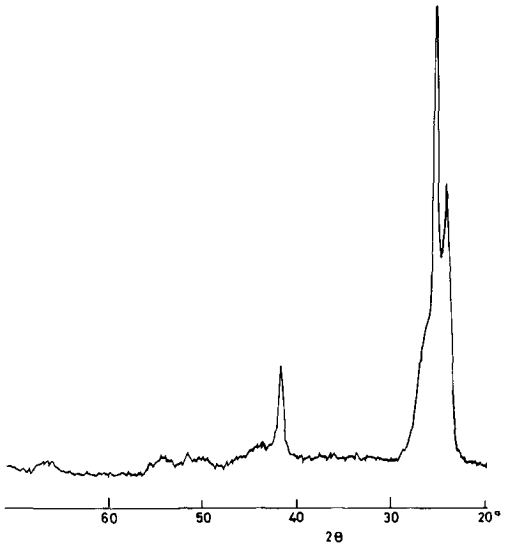

FIG. 2. X-Ray diffractogram. Al_2O_3 + $AlPO_4$ (1/1) after 1000°C, 3 h treatment.

Texture

Particle size. The more relevant statistical dimensions calculated from the particle size distribution measurements are collected in Table 2. Counting was accomplished between 2.74 and 60 μm in 14 channels at a 1.2 ratio, with an orifice diameter of 140 μm. No relevant differences between samples were observed.

Also, SEM (Fig. 4) showed no important differences among the three samples. The texture was mainly amorphous, with pore openings greater than 200 Å (Series I). In some cases, some poorly defined microcrystalline particles were apparent on the surface; their size in sample F was about double that in B and PC (Series II). They probably signalled an incipient crystallization which can be followed by XRD as temperature increases.

Specific surface area, S_{BET}. From the nitrogen adsorption–desorption isotherms (Fig. 5) at 77 K, in the range $p/p_0 < 0.3$, S_{BET} values have been obtained. They are given in Table 3, together with the more relevant textural parameters of the samples. The C_{BET} values, not far from 100, are similar to those for inorganic oxides. They denote a high heat of adsorption, and were employed, after Lecloux (*17*), for determining the pore size distribution.

TABLE 2

Particle Size Statistical Diameters (μm)

Sample	Mean	Median	Mode
B	7.5	28	25
F	6.6	22	31
PC	6.6	24	20

Porosity. Macro and mesoporosity data from mercury penetration porosimetry are given in Fig. 6. From these curves a high incidence of macroporosity in the total pore volume of all samples is apparent. Macropores larger than 13 μm are present in samples B (65%) and PC (42%), as well as pores smaller than 180 Å (24 and 30%, respectively). Sample F is essentially mesoporous; only 16.5% of its volume is in pores >13 μm, and it does not show porosity under 62 Å. A summary of these data is given in Table 3 (column 4).

The analysis of N_2 isotherms for mesoporosity studies was made according to Broekhoff (*16*). All three isotherms belong to BDDT type IV with an HI hysteresis which is not well defined at high pressures in sample F, and a fairly wide distribution of pore sizes. The nearly parallel aspect of the two branches over an appreciable range

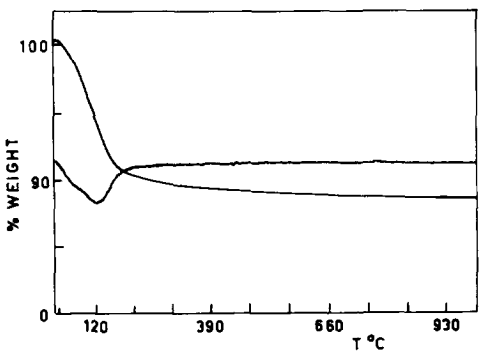

FIG. 3. Aluminum phosphate, sample B, TG, and DTG. Static air atmosphere, 10°C/min scan rate.

SERIES I

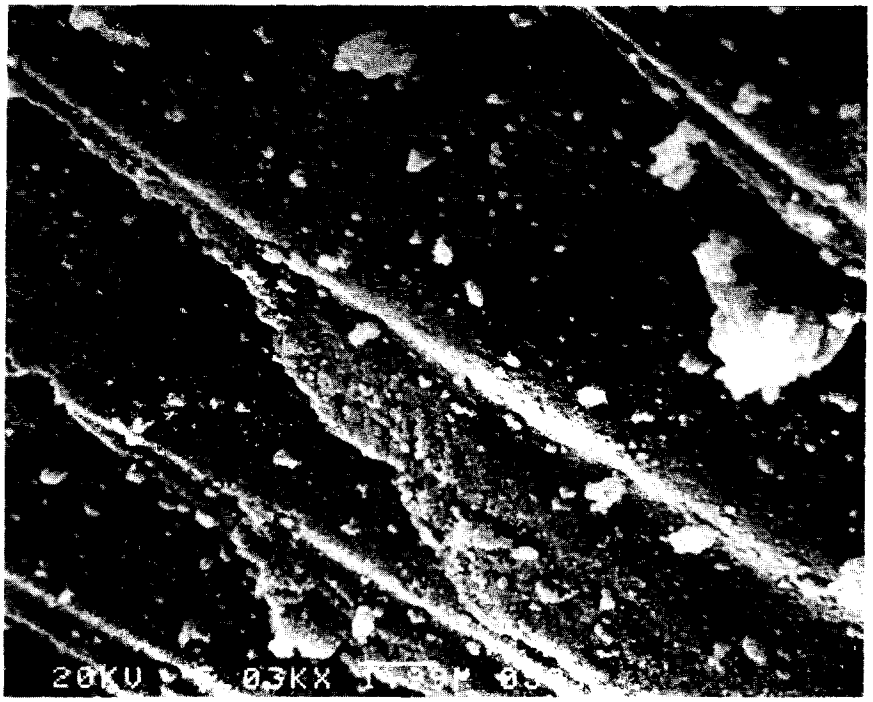

SAMPLE B x 5000

SERIES I

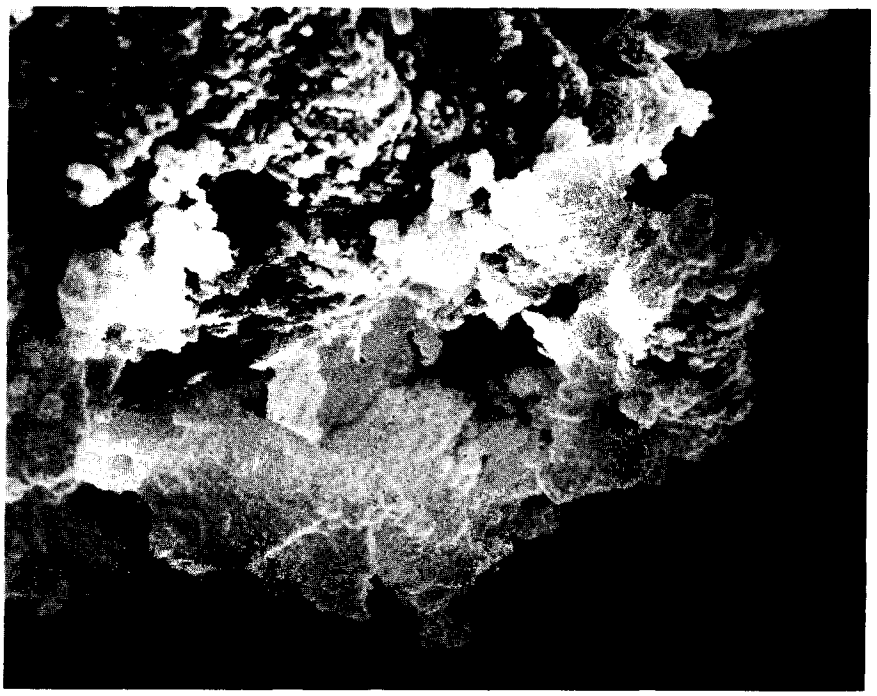

SAMPLE F x 5000

FIG. 4. Scanning micrographs. Series I × 5000, samples B, F, PC. Series II × 20,000, samples B, F; × 40,000, sample PC.

SERIES I

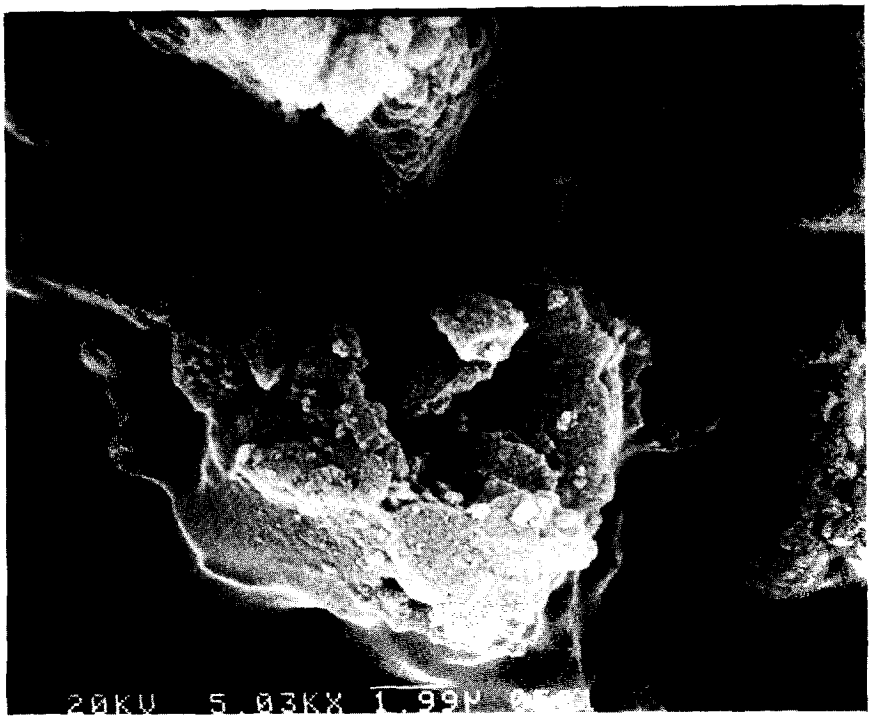

SAMPLE PC x 5000

SERIES II

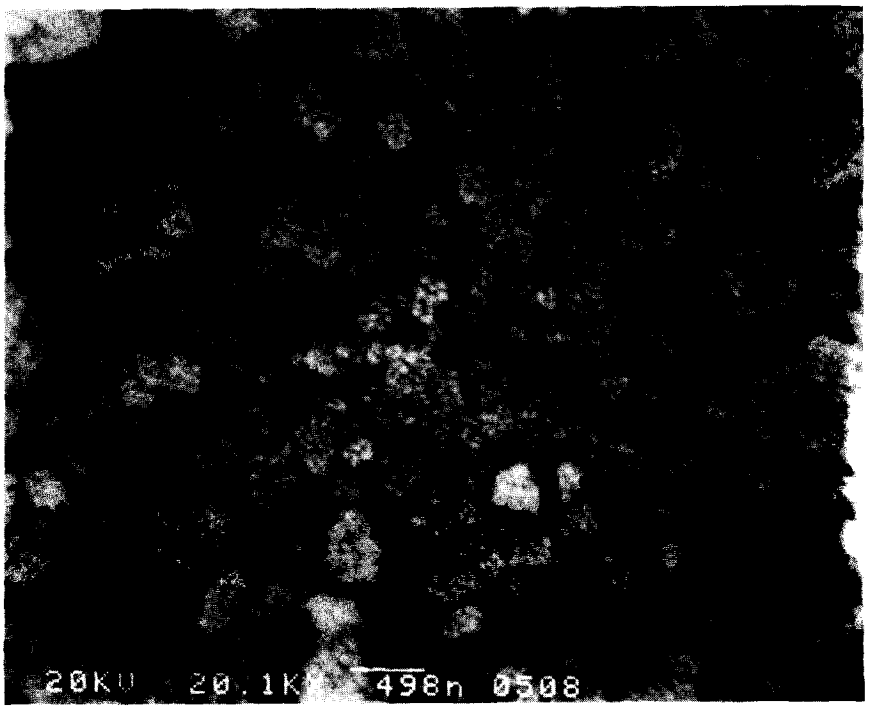

SAMPLE B x 20000

FIG. 4—*Continued.*

SERIES II

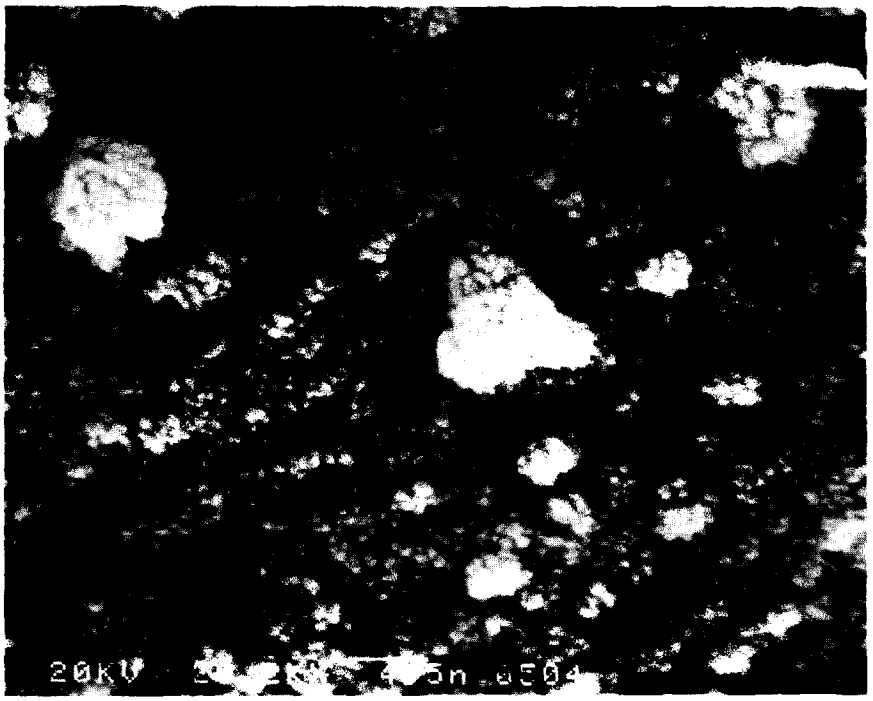

SAMPLE F x 20000

SERIES II

SAMPLE PC x 40000

FIG. 4—*Continued.*

TABLE 3

Textural Parameters

Sample	S_{BET} ($m^2\ g^{-1}$)	C_{BET}	Hg porosim.	Nitrogen isotherms			t Curves				
			$V_{p(d>60\ Å)}$ ($cm^3\ g^{-1}$)	$V_{p(600>d>20)}$ ($cm^3\ g^{-1}$)	Diameter, Å		Hyst. p/p_0	Cond. p/p_0	S_t ($m^2\ g^{-1}$)	$V_{p(d<20\ Å)}$ ($mm^3\ g^{-1}$)	d_{av} (Å)
					Mode	Mean					
B	257	82	1.087	0.711	93	94	0.55	0.50	244	9.3	169
F	156	72	0.966	0.627	115	137	0.42	0.42	139	0.9	248
PC	271	69	1.310	0.926	115	113	0.55	0.48	268	3.4	193

of relative pressures is associated with cylindrical pores or with voids formed upon contact of near spherical particles. Unsaturation in sample F points to the presence of a developed macroporosity, confirmed by mercury penetration.

The SEM micrographs, together with XR diffractograms and N_2 isotherms, lead us to conclude that the texture of the samples may be formed mainly by cylindrical or spheroidal pores located in the amorphous phase, with no apparent crystallinity in them.

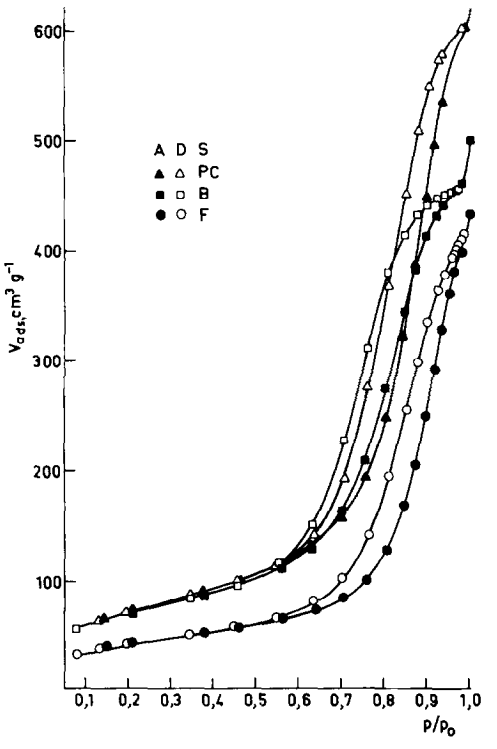

FIG. 5. N_2 adsorption–desorption isotherms. (■) Sample B, (●) sample F, (▲) sample PC.

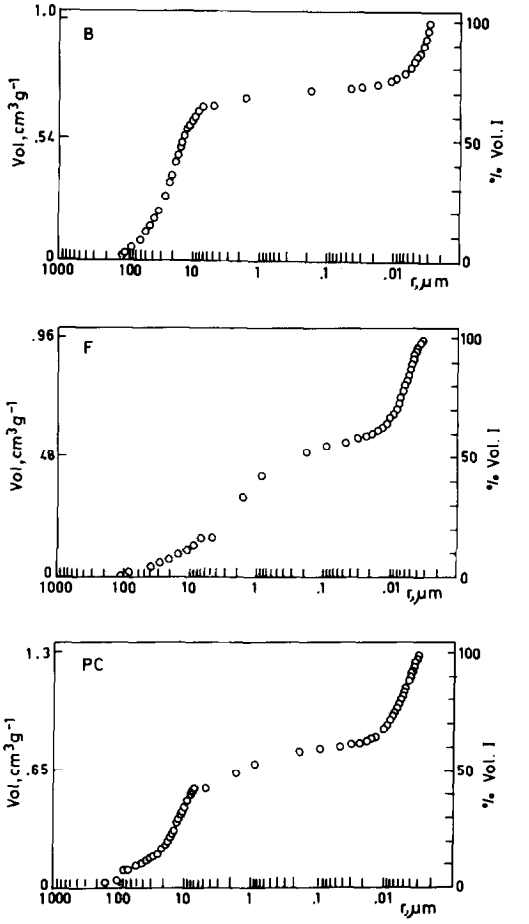

FIG. 6. Mercury penetration porosimetry. Samples B, F, PC.

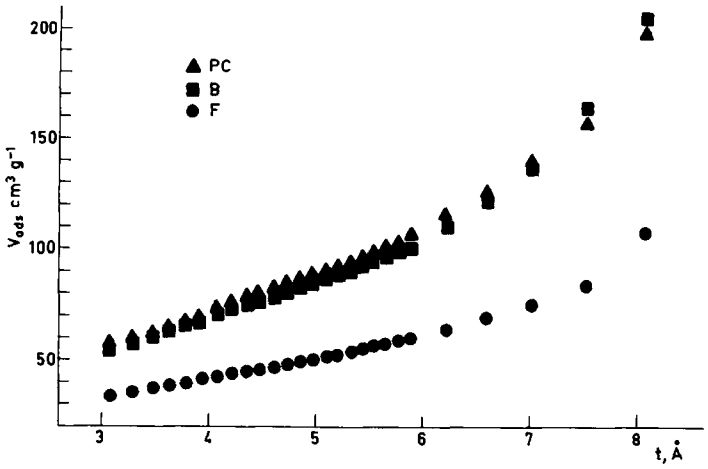

FIG. 7. *t*-Plots. (■) Sample B, (●) sample F, (▲) sample PC.

The mesopore volume was obtained from the quantity of gas adsorbed at $p/p_0 = 0.98$ (column 5 in Table 3). The *t*-plots (*17*) of the adsorption branch of the isotherms are shown in Fig. 7. From them, a weak microporosity, almost null in sample F, is apparent. In samples B and PC capillary condensation starts at relative pressures lower than the closure of the corresponding hysteresis loops, showing a small incidence of sites in which reversible condensation occurs (Table 3, columns 8 and 9). Surface areas from the *t*-plot (column 10) correspond quite well with S_{BET} data.

By application of Brunauer's (*18*) modeless method and cylindrical pore shape model to the adsorption branch of the isotherms, calculations of pore size distributions have been made. The curves (percentage frequency versus mean pore diameter) are shown in Fig. 8. From them and through application of elemental statistical calculus, mode and mean pore diameter have been obtained (Table 3, columns 6 and 7). In the last column, an average diameter ($d_{av} = 40{,}000\ V_{pHg}/S_{BET}$) is also given.

From those data, some differences in textural parameters of the three samples are apparent. Especially, sample F, precipitated from ammoniacal medium, shows an important departure in S_{BET} and pore size distribution from samples B and PC which were obtained with ethylene and propylene oxide, respectively.

Thus, not only pH, but also the nature of the precipitating solution plays a major role in the textural characteristics of the near stoichiometric aluminum phosphates obtained. This influence would be probably due to the entrapment of molecules of the media by the precipitated amorphous mass

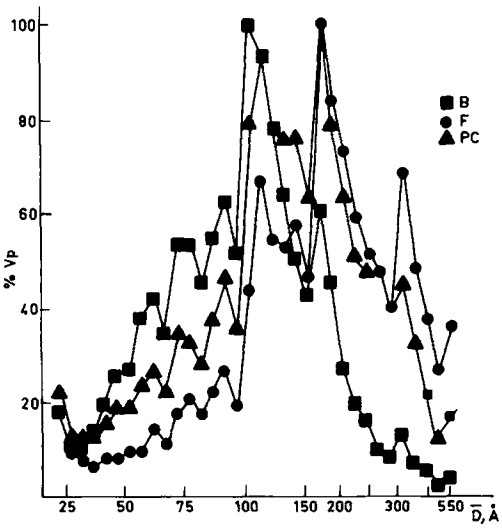

FIG. 8. Pore diameter distributions. Percentage of maximum pore volume versus average pore diameter, Å. (■) Sample B, (●) sample F, (▲) sample PC.

TABLE 4

Water Loss TG Data

Sample	% Weight losses		OH (nm^2)
	Total	275–1000°C	
B	11.65	1.25	3.26
F	13.67	1.66	7.11
PC	10.25	0.89	2.20

in the first stages of preparation, followed by corresponding gas evolution as heating to 650°C proceeds. In this way, macroporosity could be related to physical properties of the precipitating agents, and meso and microporosity with OH^- losses, as thermoanalyses will show later, and with the appearance of crystallinity.

Surface Reactivity

IR spectra. They are similar for all three samples. Peaks are not well developed; only those corresponding to O—P—O (485, 602–613 cm^{-1}), Al—O in combination with P—O (709 cm^{-1}), and P—O (1114, 1254 cm^{-1}) (*19*) are apparent. A shoulder at 2926 cm^{-1} and a peak at ~1460 cm^{-1} for the F sample, probably related with the aqueous ammonia precipitation medium of the aluminum phosphate, is the only difference observed in the three spectra. This difference has been emphasized through proper treatment of the spectra, which shows, besides, a higher content of O—P—O and Al—O groups probably affected by H-bonding to their O atom with other more abundant surface OH groups.

Surface hydroxyl content. From the TG and DTG curves obtained for all three samples after equilibration for 1 week in a desiccator, the percentage total losses and OH^- content corresponding to the continuous weight loss between 275 and 1000°C, were calculated (Table 4).

The higher crystallinity and lower surface area of sample F revealed through XRD and adsorption measurements are not confirmed by these data, which, on the contrary, agree with the small differences between samples observed in the IR spectra.

Surface chemical properties. Data on the adsorbed amounts, X_m, in meq/g, of the three titrant amines used in the present work, are given in Table 5. The total number of acidic centers deduced from adsorption of cyclohexylamine ($pK_a \sim 10.6$) are comparable with those previously reported from butylamine ($pK_a \sim 10.73$) adsorption by Kearby (*9*) and Tada and co-workers (*20*), and one half the value found from ammonia adsorption by Gallace and Moffat (*5*). As has been said elsewhere (*14, 15*), the tabulated X_m values are a function not only

TABLE 5

Titrant Adsorption (298 K, Cyclohexane)

Titrant	pK_a	meq/g			Sites/nm^2		
		B	F	PC	B	F	PC
CY	10.6	0.789	0.815	0.995	1.844	3.147	2.211
DTBMPY	7.5	0.090	0.049	0.057	0.311	0.189	0.127
PY	5.3	0.320	0.190	0.227	0.750	0.734	0.504
PH	9.9	0.055	0.110	0.077	0.129	0.425	0.172
DTBNPH	11.7	0.002	0.001	0.002	0.0045	0.004	0.0042
PNTZ	(IE)7.13	0.002	0.0002	0.002	0.0045	0.0008	0.0042
DNB	(EA)2.21	0.003	0.001	0.001	0.0072	0.0039	0.0034

Note. IE, ionization energy; EA, electron affinity.

of amine pK_as, but also of their molecular size due to steric hindrance within the pore system of the solid, as can be seen through a comparison of data for DTBMPY (pK_a 7.5, A = 136 Å^2) and PY (pK_a 5.3, A = 39 Å^2), and the corresponding sample pore sizes in Table 3.

As it is known, the structure of aluminum phosphate is such that both atoms, phosphorus and aluminum, are surrounded by a tetrahedron of oxygen atoms. It is isostructural with SiO_2 with P and Al atoms alternating regularly in the network of corner-linked oxide tetrahedra. When the preparation is rich in phosphorus, segregation of P_2O_5 as a separate phase takes place (*4*); on the contrary, Al_2O_3 is present when Al/P > 1. In this work, however, no apparent independent phase has been shown by X-ray diffraction, although, their presence in quantities lower than the detection limit of the technique cannot be discarded, thus justifying the found differences in acidity and/or basicity of the samples. In fact if the Al/P ratio were 1 in all three samples, only differences in crystallinity (size of crystals, surface defects, ratio of amorphous to crystalline phase) could explain the different amine adsorption behaviour, since the final precipitation pH was similar.

In our opinion, the resulting acidity seems a combination of two factors: surface OH^- content and P/Al ratio. The former, as Campelo *et al.* (*26*) stated, is related to the degree of order of the crystalline structure, and consequently to its electron transfer properties. According to Moffat (*2*), an increasing value of the P/Al ratio diminishes acidity in the studied range. A proper combination of the two factors may explain the obtained results at pK_a ~ 10.6. The P/Al ratio is mainly responsible for those corresponding to strong acid sites, as Peri (*21*) pointed out for exposed Al atoms in the Al—O—P surface links.

Some previous work on basic sites in $AlPO_4$ has been made by Gallace and Moffat (*5*) and by Haber and Szybalska (*4*). Also Peri observed, by adsorption of CO_2 and HCl on $AlPO_4$, a small presence of "α-sites" or reactive surface oxides ions. Our results for phenol adsorption show a certain surface concentration of basic centers (see Table 5) which is about one order of magnitude lower than that of acidic ones.

A comparison between adsorbed amounts and corresponding pK_a's for acid and base titrants, shows that acid sites are much more numerous than basic ones and the acid strength is more important, as Peri (*21*) has suggested. Again, sample F shows an important difference in basic sites content with respect to the other two samples, almost doubling their B/A ratio. Since the oxygen exposed atoms are responsible for the basicity of the samples, the higher relative number of surface oxygen in sample F compared to B (more Al) and PC (more P) may be responsible for such a situation. Alternatively, following Moffat (*22*), the NH_4OH or HOH retained by the sample (TG and IR data) on phosphorus or aluminum atoms, may enhance the basic capabilities of the bridging oxygen atoms in the P—O—Al linkages, thus explaining the obtained results. Results with DTBMPH, not paralleling those with DTBMPY, reinforce that supposition if ammonia and/or water are retained in the narrower and, for this titrant, unreachable pores.

One-electron donor and one-electron acceptor properties were determined on the basis of adsorption on the solid surface of 1,3-dinitrobenzene (DNB, EA = 2.21 eV) and phenothiazine (PNTZ, IE = 7.13 eV) as indicated. Results are given in Table 5.

Although the exact nature of the sites involved in the electron transfer processes is not clear, the oxidizing sites were identified (*23, 24*) as Lewis acid sites or polarity defects related with Al^{3+}, whereas the reducing centers were ascribed to basic OH^- surface groups or cationic vacancies in the vicinity of O^{2-}. In some cases the simultaneous presence of both sites has been shown (*24, 25*). Thus, PNTZ adsorption can be related with acidity lower than 7.5 pK_a, and that of DNB with basicity of the samples.

Anyway, from Table 5, concentration of electron transfer sites on $AlPO_4$ surface is so extremely low, that it is difficult to establish a relationship with acid and basic centers. It seems clear, however, that basicity in sample F like in (*26*) lacks completely reducing capacity, thus maintaining DNB adsorption in it as low as in B and PC samples.

CONCLUSIONS

From this study the relationship between preparation pH and Al/P ratio with the nature of the resultant $AlPO_4$ is beyond question. Also the precipitating agent seems to play an important role, at least with samples treated at temperatures at which total crystallinity has not yet been attained. Thus, in working with ammonia and ethylene and propylene oxides, not only differences in surface area and pore size distribution have been shown, but also, and more important, in acid site/basic site ratio as well as in one-donor, one-acceptor electron properties. In that sense, the nature of the precipitant agent could be a new clue in the design of catalysts with a required reactivity.

Anyway, further study is needed to ascertain the influence of these changes in the final behavior of the solids, and to obtain more general conclusions.

REFERENCES

1. Marcelin, G., Vogel, R. F., and Swift, H. E., *J. Catal.* **83,** 42 (1983).
2. Moffat, J. B., *Catal. Rev. Sci. Eng.* **18,** 199 (1978).
3. Itoh, H., Tada, A., and Tanabe, K., *Chem. Lett.*, 1567 (1981).
4. Haber, J., and Szybalska, U., *Discuss. Faraday Soc.* **72,** 263 (1981).
5. Gallace, B., and Moffat, J. B., *J. Catal.* **76,** 182 (1982).
6. Itoh, H., Tada, A., and Hattory, H., *J. Catal.* **80,** 494 (1983).
7. Haggin, J., *Chem. Eng. News* **13,** 9 (1982).
8. Wilson, S. T., Lok, B. M., Messina, C. A. Cannan, T. R., and Flanigen, E. M., *J. Amer. Chem. Soc.*, **104,** 1146 (1982).
9. Kearby, K., *in* "Proceedings, 2nd International Congress on Catalysis, Technip, Paris," p. 2567. 1961.
10. Alberola, A., and Marinas, J. M., *An. Real Soc. Esp. Fís. Quím., Ser. B* **65,** 1000 (1969).
11. Vogel, R. F., and Marcelin, G., *J. Catal.* **80,** 492 (1983).
12. Moffat, J. B., and Gallace, B., *J. Catal.* **80,** 496 (1983).
13. Campelo, J. M., García, A., Gutierrez, J. M., Luna, D., and Marinas, J. M., *Canad. J. Chem.* **61,** 2567 (1983).
14. Marinas, J. M., Jiménez, C., Campelo, J. M., Aramendia, M. A., Borau, V., and Luna, D., *in* "Proc. 7th Symp. Iberoamericano Catal. La Plata, Argentina," p. 79. 1980.
15. Campelo, J. M., García, A., Luna, D., and Marinas, J. M., *Afinidad* **39,** 325 (1982).
16. Broekhoff, J. C. P., *in* "Preparation of Catalysts II" (B. Delmon, P. Grange, P. Jacobs, and G. Poncelet, Eds.), p. 663. Elsevier, Amsterdam, 1979.
17. Lecloux, A., and Pirard, J. P., *J. Colloid Interface Sci.* **70,** 265 (1979).
18. Brunauer, S., Mikhail, R. S., and Bodor, E. E., *J. Colloid Interface Sci.* **25,** 353 (1967).
19. Farmer, V. C., *in* "The Infrared Spectra of Minerals" (V. C. Farmer, Ed.). London, 1974.
20. Tada, A., Yoshida, M., and Hirai, M., *Nippon Kagaku Kaishi*, 1379 (1973).
21. Peri, J. B., *Discuss. Faraday Soc.* **52,** 55 (1971).
22. Moffat, J. B., Vetrivel, R., and Viswanathan, B., *J. Mol. Catal.* **30,** 171 (1985).
23. Flockhart, B. D., Leith, I. R., and Pink, R. C., *Trans. Faraday Soc.* **65,** 542 (1969).
24. Flockhart, B. D., Leith, I. R., and Pink, R. C., *Trans. Faraday Soc.* **66,** 469 (1970).
25. Campelo, J. M., García, A., Gutierrez, J. M., Luna, D., and Marinas, J. M., *Colloids Surf.* **8,** 353 (1984).
26. Campelo, J. M., García, A., Gutierrez, J. M., Luna, D., and Marinas, J. M., *J. Colloid Interface Sci.* **95,** 544 (1983).